ISRS

Multi-sensor Approach for the Estimation of Above-Ground Biomass of Mangroves

Humaira Sanam[1] · Anjana Anie Thomas[2] · Arun Prasad Kumar[2] · Gnanappazham Lakshmanan[1]

Abstract

Mangroves are woody halophytes thriving in muddy substratum along the coastal areas of the tropics and sub-tropics. They are often credited for their exceptional carbon sequestration capability. Estimating above-ground biomass (AGB) through field survey is tedious, particularly in a hostile environment like a mangrove ecosystem. However, the quantification of AGB is made possible with the help of continued advancements in sensor technology and computational algorithms. This research attempts to model the AGB of mangroves present in Bhitarkanika, Odisha, using a multi-sensor approach. We utilized multispectral Sentinel-2 (SM) and Landsat-8 (LO), and hyperspectral Airborne Visible Infra-Red Imaging Spectrometer—Next Generation (AN) datasets in our analysis. The mangrove biomass was calculated for 42 sample plots from a field survey using species specific and common allometric equations. After data-specific preprocessing; six feature sets namely reflectance bands, band ratios, vegetation indices (VIs), texture-based Gray Level Co-occurrence Matrix (GLCM) features of reflectance, band ratios and VIs were extracted for each dataset. The co-located set of features derived from each dataset were regressed against the AGB estimated using field methods of 42 sample plots (1) independently for each feature set, (2) in a combination of feature sets for each dataset and (3) in a combination of the feature sets of all three datasets as a multi-sensor approach. Feature selection techniques were used to get the best possible output of combined AN, SM and LO datasets. The results show that the combination of textural features gave better prediction models than independent sets of features. Also, Genetic Algorithm (GA) and Recursive Feature Elimination CV (RFECV) proved to be better feature selectors than other classical approaches. AN, SM and LO resulted in the R^2 value of 0.41, 0.85 and 0.35 with RMSE of 356.81, 195.49 and 366.84 t/ha, respectively; while, the multisensory approach yielded a maximum R^2 value of 0.7 and RMSE of 244.86 t/ha. The results show that the structural information of vegetation canopy obtained from textural parameters of different input bands has improved the regression model to predict the biomass.

Keywords Mangroves · Above-ground biomass · Multi-sensor · Hyperspectral · GLCM · Genetic algorithm

✉ Gnanappazham Lakshmanan
gnanam@iist.ac.in

Humaira Sanam
humairasanam7@gmail.com

Anjana Anie Thomas
anjanaanie999@gmail.com

Arun Prasad Kumar
arunprasad@cutn.ac.in

[1] Department of Earth and Space Science, Indian Institute of Space Science and Technology, Valiamala P.O., Thiruvananthapuram, Kerala 695 547, India

[2] Department of Geography, School of Earth Sciences, Central University of Tamil Nadu, Thiruvarur, Tamil Nadu 610 005, India

Introduction

Mangroves have several characteristic features that separate them from other woody plants. Mangroves are halophytes with unique breathing roots—pneumatophores. There are 110 species of mangroves present, of which 54 species are true mangroves, and the rest are associated mangroves. Mangroves help recycle nutrients; act as a link between terrestrial and marine habitats, thus supporting various life forms (Nagelkerken et al., 2008); serve as a sink for different minerals (Alongi et al., 2004) and sequester a considerable percentage of global carbon annually (Bouillon et al., 2008; Kristensen et al., 2008; Alongi & Mukhopadhyay, 2015). Mangroves are degrading fast due to various anthropogenic activities. UNEP (United Nations Environmental

Programme) launched the "Blue Carbon Initiative" project to protect and restore mangroves and other vegetation.

Remote sensing offers ample scope for frequently monitoring these salt marshes without difficulty and with good precision. Remote sensing can help determine the biophysical parameters for a vast area in a short time. Multispectral remote sensing views a region in a few wide wavelength bands but can range from medium to very high spatial resolution. Hyperspectral remote sensing is a kind of remote sensing that uses a range of wavelengths from the electromagnetic spectra by dividing it into bands of very fine narrow wavelengths so that variation in spectral properties of different species can be studied and determined precisely for proper identification and discrimination of species as well as determination of their biophysical and biochemical parameters.

Biomass is the biophysical property indicative of the carbon sequestration capability of mangroves. It is the measurement of the content of the living tissue mass present per unit area (e.g., g/m^2). Researches across the world prove that mangroves can sequester 5% of the carbon in the atmosphere even though they cover only 0.1% of the earth's surface area (Alongi, 2002). Earlier biomass calculation was possible only by destructive methods or by measuring the trees' biophysical parameters and using species-specific or standard allometric equations. With the advances in remote sensing, methods were adopted to estimate the biophysical properties of vegetation that involve in situ data collection of the biophysical variables and then model the biomass using features derived from remotely sensed satellite images (Hirata et al., 2014; Patil et al., 2014; Green et al., 1998; Kovacs et al., 2009; Fatoyinbo et al., 2008). Studies have been done in the past to link biomass values with values of Vegetation Indices (VIs). VIs are the mathematical transformation of the spectral bands that assess the spectral contribution of objects to different bands of the electromagnetic spectrum (Elvidge & Chen, 1995). VIs minimize external effects such as sun angle, sensor angle, shadow, soil background, leaf and canopy angle and terrain effect (Kasawani et al., 2010). Sarker & Nichol (2011) tested ten slope-based and eleven distance-based vegetation indices derived from the AVNIR-2 sensor. They compared them with other models (texture-based and band ratio-based) for biomass estimation. Eckert (2012) and Zhu et al. (2015) also used VIs derived from WorldView data for mangrove biomass estimation. VIs like NDVI that are computed using red and NIR bands and have been used to estimate vegetation biomass have a limitation of saturating at high biomass levels. Some narrow-band VIs, like TVI and MNDVI, have performed reasonably well in literature in estimating biomass. At high canopy density, narrow-band indices involving red edge bands have been more accurate in estimating AGB (Mutanga & Skidmore, 2004).

Apart from directly using VIs, other features derived from VIs can also be used to study the biophysical parameters. In remote sensing, the texture is a function of spatial variation of the brightness intensity of the pixels (Armi & Fekri, 2019). It is defined as the function of local variance of the spatial resolution in the image and also depends on the size of the objects in the scene (Haralick et al., 1973; Woodcock & Strahler, 1987). Texture of an image depends upon three characteristics: (1) repetition of some local order that is larger than the order's size, (2) the order consists in the systematic arrangement of elementary parts and (3) the parts have approximately same dimensions in the textured region (Tuceryan & Jain, 1993). Texture analysis in remote sensing depends on the structure and statistics of the pixels (Haralick, 1979). Texture has often played a more critical role than reflectance measurements for high-resolution images (Boyd & Danson, 2005; Podest & Saatchi, 2002; Ulaby et al., 1986; Dell'Acqua & Gamba, 2006). The size and the spacing of the tree crowns determine the texture of an image of a forested area (Nichol & Sarker, 2010).

Several statistical models such as linear regression with or without log transformation (Steininger, 2000; Calvao & Palmeirim, 2004); multiple regression models (Eckert, 2012; Dobson et al., 1995; Hyde et al., 2007); nonlinear regression (Santos et al., 2003); artificial neural networks (Foody et al., 2001; Zhu et al., 2015) and semi-empirical models (Castel et al., 2002) have been used in earlier studies to model the AGB. The multiple regression model is considered the best among the other models as it has proved to reasonably establish some relationship between the field biomass and remote sensing-derived information (Hame et al., 1997; Kurvonen et al., 1999; Hyde et al., 2007; Nichol & Sarker, 2010; Sarker & Nichol, 2011).

The main objective of our study is to model the Above Ground Biomass of Bhitarkanika mangroves using features derived from remotely sensed data of three different sensor types of namely high resolution multispectral, coarse resolution multispectral and high spatial and spectral resolution hyperspectral data. It compares the results obtained by applying the multilinear regression machine-learning algorithm to different feature combinations of reflectance bands and their textures. The study investigates the importance of textural features in relation to high spatial resolution imagery in modeling biomass. This may help in the future to accurately estimate mangrove biomass remotely. The study also inspects the role played by the spatial and spectral resolutions in modeling biomass. Attempts are also made to combine features from all the datasets using a multi-sensor approach to assess improvement in biomass estimation. In this process, we used various feature selection methods and compared their feature selection potential in getting the best possible outcomes.

Study Area

This study explores the relationship between the ground truth biomass data and the satellite-derived features of the mangroves of the Bhitakanika National Park, a 145 km² large national park in the Kendrapara district, Odisha, India. Our study area extends from 20° 38′ 19″ N to 20° 47′ 27″ N latitudes and 86° 49′ 26″ E–87° 05′ 48″ E longitudes. In 1998, this area got the designation of National Park, and in 2002, it obtained the status of a Ramsar site. Three major rivers of northeast India—Brahmani, Baitrani and Dhamra; combinedly make up its vast and fertile alluvial deltaic region. It is rich in biodiversity and houses rare and endangered species. It houses the Olive Ridley sea turtles and is also the breeding place of endangered saltwater crocodiles. It serves as the habitat of more than 200 species of birds and is a host of several migratory birds. Among the numerous reptiles, mammals and vertebrates, commonly found are the cobras, the pythons, otters, spotted dear, the endangered water monitor lizards, Fishing Cat, etc. (Ravishankar et al., 2004). Its proximity to the Bay of Bengal makes its soil saline, making the area rich in different species of mangroves. The sanctuary also has backwater, mud flats, tidal creeks and distributaries of many rivers and ramifying streams, making it a land of unique flora and fauna. It has 32 true species and 46 associated species of mangroves. The major species found here are *Avicennia marina, Avicennia officinalis, Ceriops decandra, Exoecaria agallocha, Heritiera fomes, Kandelia candel, Sonneratia apetala, Sonneratia caseolaris, Xylocarpus granatum,*, and *Xylocarpus moluccensis*. The only endemic species present in the sanctuary is *Heritiera kanikensis* (Majumdar & Banerjee). Semi-diurnal tides inundate the area (Fig. 1).

Materials

Satellite/Sensor Images

Features for developing the biomass model were derived from three different satellite images (Table 1). First is a coarse resolution image from the multispectral Landsat 8 Operational Land Imager (OLI) hereafter named as LO acquired on 26th November 2015. It provides data in 10 multispectral bands with a spatial resolution of 15 m for the panchromatic band to 30 m and 100 m for the multispectral bands. The second image is from high spatial and spectral resolution—Airborne Visible Infra-Red Imaging Spectrometer—Next Generation (AVIRIS-NG), a hyperspectral optical sensor of Jet Propulsion Laboratory (JPL), NASA, that was on board an ISRO B200 aircraft and a part of the ISRO-NASA airborne campaign. These data, hereafter named as AN in this manuscript, provide high-resolution airborne imaging over broad spectra in very narrow wavelength channels, the spectral resolution being 5 nm and spatial resolution of about 4 m over 420 narrow spectral bands. The narrow bandwidth gives precise information about subtle changes in the reflectance and absorption features (Chaube

Fig. 1 Study area map showing Sentinel 2 false color composite (NIR, Red and Green bands) of Bhitarkanika, Odisha with locations of field plots
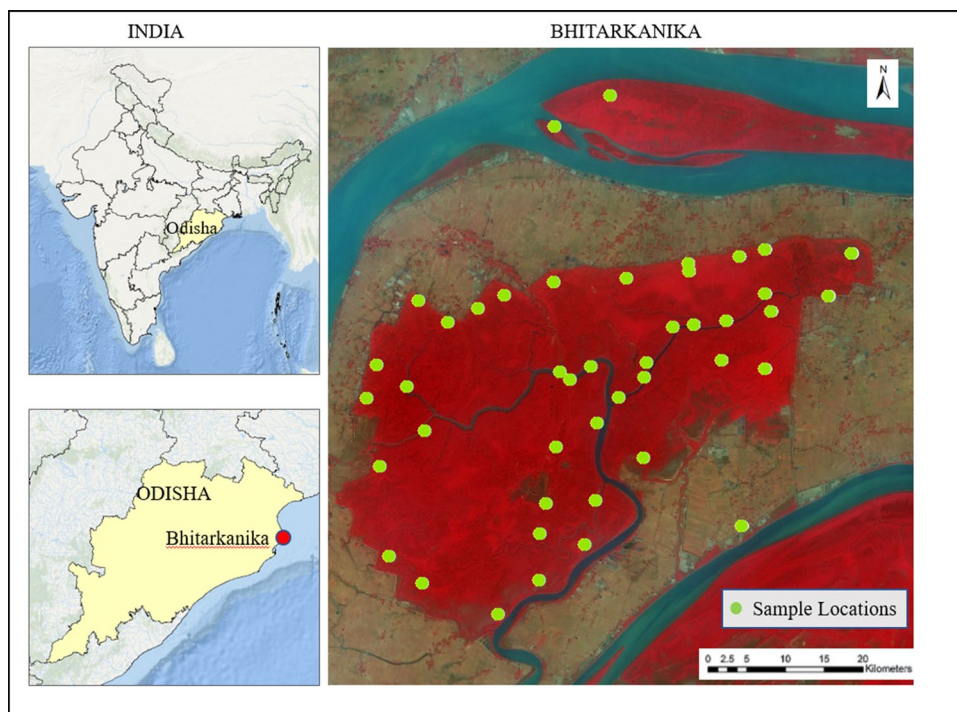
Table 1 Spectral specifications of LO, SM and AN dataset used

Landsat-8 OLI			Sentinel-2A MSI			AVIRIS-NG		
Central wavelength (nm)	Band width (nm)	Spatial resolution (m)	Central wavelength (nm)	Band width (nm)	Spatial resolution (m)	Wavelength range (nm)	Band width (nm)	Spatial resolution (m)
482.5	65	30	492.4	66	10	400–2450	5 nm for each of the 420 bands	4
562.5	75	30	559.8	36	10			
655	50	30	664.6	31	19			
865	40	30	704.1	15	20			
1610	100	30	740.5	15	20			
2200	200	30	782.8	20	20			
			832.8	106	10			
			864.7	21	20			
			1613.7	91	20			
			2202.4	175	20			

et al., 2019). AN data for the study area was acquired on 26th and 28th December 2015. We also utilized a medium-resolution Copernicus Sentinel-2 Multispectral Instrument (MSI) image hereafter named as SM, of 1st January 2016 that was close to AN acquisition time, provides spatial resolutions varying from 10 to 60 m over broader multispectral channels. SM imagery collects data in thirteen multispectral bands, of which three are vegetation red edge bands, one is NIR (Near-InfraRed) band and three are SWIR (Short Wave InfraRed) bands (one is SWIR-cirrus) that help in the detailed monitoring of vegetation and parameter generation.

In situ Data

The field biomass variables from sample plots were collected during two time periods—December 2012 and April 2013. The in situ data were collected from 42 stratified sample plots selected based on the existing mangrove community map (SAC, 2012) distributed in the mangrove forest of Bhitarkanika. The sample plots were of size 10 m × 10 m. All sample plots were selected far from roads, creeks, or other interventions, well within the vegetated area. Biophysical parameters like DBH was measured using measuring tape and tree height was measured using the Leica Disto D8 LASER distometer. The number of trees in each species was recorded with the input of field experts from the Forest Department, State Government of Odisha, India.

Methodology

Preprocessing of the Images

AN is an imaging spectrometer, and it needs to be spectrally and radiometrically calibrated prior to data analysis.

According to NASA—'All AVIRIS-NG data is processed by the AVIRIS-NG instrument ground data system (IGDS) at JPL.' This rectifies the errors due to the aircraft's motion and frees the data from geometric and radiometric errors caused due to the atmospheric effects. The orthorectified and atmospherically corrected reflectance data by using ATREM with simultaneous three phase H_2O removal from AN data product is used in this study (Bue et al., 2015). The study area is covered under five adjacent AN image scene. Hyperspectral data comes in several narrow contiguous bands; not all bands contain extractable information. The bad bands were manually checked and removed before working with the data. Further, considering the computational complexity of the hyperspectral aerial dataset, the image features are indented to be derived from the local neighborhood region of sample plots. Hence, a buffer region of 200 m around samples are considered for further analysis. Histogram matching was performed for all the five scenes prior to the mosaicking of the scenes. Google Earth Engine was used to get the preprocessed reflectance data of both Landsat-8 (LO) and Sentinel-2 (SM).

Feature Extraction

The images are processed, and the features are extracted from each of the three images for further processing and analysis (Fig. 2). The extracted features are a combination of (1) reflectance bands, (2) vegetation indices, (3) band ratios and (4) GLCM parameters of a set of above.

Reflectance Bands

The bands mentioned in Table 1 for SM and LO multispectral imagery have been considered for the data analysis. AN has 420 bands, and using all the bands in the study can make
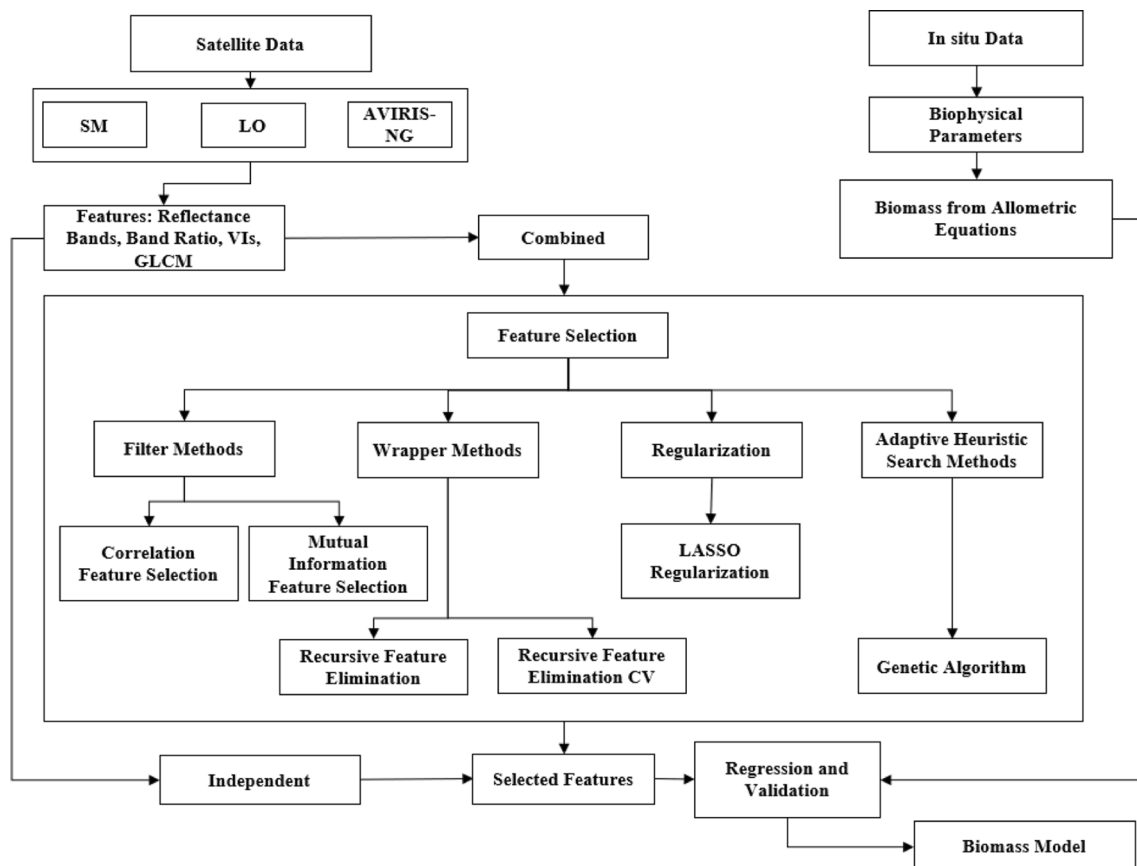
Fig. 2 Flowchart showing the methodology for independent and multi-sensor approach for biomass modeling

the feature size bulky and hard to process. Moreover, all the bands may not contribute to the estimation of mangrove biomass. A total of 12 reflectance bands were selected which are represented by vegetation indices and the highest slope change from the first derivative of the spectra (Prasad & Gnanappazham, 2014) that include wavelengths of 552, 682, 707, 717, 862, 972, 1083, 1193, 1263 and 1473 nm.

Vegetation Indices

In the present study, 12 Vegetation Indices (VIs) are calculated from the SM and 11 from LO multispectral images to model the biomass using multiple regression analysis. AN being hyperspectral data has a greater number of narrow bands. Thus, we have chosen VIs that are common to our other two datasets and additional VIs corresponding to the reflectance bands selected for our hyperspectral imagery. A total of 20 VIs are calculated for the AN image.

Textural Features

Even though VIs reduce the atmospheric effects and noise, they often suffer from the problem of saturation at high biomass levels. So, we try to explore the potential of textural parameters to improve the biomass estimation (Kuplich et al., 2005; Prasad, 2016).

Grey Level Co-occurrence Matrix (GLCM) extracts statistical measures from pixels of an image determined by the spatial relationship between neighborhood pixels with a specific intensity. The selection of moving window size is an important factor because the small window size exaggerates the local variance, whereas the large window size may not extract textural information because of the over-smoothening of the textural variation (Chen & Gong, 2004). This study used small moving window sizes of 3×3 to estimate the 8 GLCM parameters—Mean, Variance, Homogeneity, Contrast, Dissimilarity, Entropy, Angular Second Moment (ASM) and Correlation from the following (Supplementary material. 1).

  (i) LO—(a) 6 reflectance bands, (b) 15 simple band ratios, (c) 11 Vegetation Indices

(ii) AN—(a) 12 reflectance bands and (b) 20 Vegetation Indices.

(iii) SM—(a) 9 reflectance bands, (b) 28 band ratios and (c) 12 vegetation indices.

The 12 reflectance bands and the VIs with each of their 8 GLCM parameters were considered in our study, giving a total of 288 features for the AVIRIS-NG dataset. The total number of features extracted for LO was 288 and for SM was 441. The entire output of the three sensor data was analyzed individually and combined manner after feature selection methods (Fig. 2).

Feature Selection Methods

With the available number of samples and more degrees of freedom, there are chances that the model learns noise in the data instead of the underlying patterns and relationships. To avoid overfitting and to improve the model, we adopted the following steps: (a) Feature reduction, (b) Use of a simpler model, (c) Regularize the model and (d) Cross-validation in each of the following methods.

The best feature selection algorithms are those that are stable to the addition or removal of training samples (Chandrashekar & Sahin, 2014; Haury et al., 2011; Dunne et al., 2002; Kalousis et al., 2007; Somol & Novovicova, 2010; Yang & Mao, 2011). We had limited samples, so we made statistical scores of the regression model as our judging criteria. We used the following Python-based feature selection techniques.

(a) *Filter Methods:* In this method, the selection of each feature is evaluated individually. (1) *Correlation Feature Selection (CFS):* Correlation statistics gives positive scores for features. The greater the score, the greater the relationship with the dependent variable. (2) *Mutual information (MIFS):* It is the application of information gain to feature selection. It measures the reduction in uncertainty for one variable given a known value of the other variable.

(b) *Wrapper Methods:* The search algorithm wraps the predictor to find the subset with the highest predictor performance (Chandrashekar & Sahin, 2014). Recursive feature elimination (RFE) technique is computationally easy and fast when compared to the sequential forward and backward selection and exhaustive elimination methods (Venkatesh & Anuradha, 2019). This algorithm runs recursively, considering the smaller and smaller set of features. Their importance is obtained using the feature importance attribute. The minimum required features are defined by the user.

(c) *Embedded Methods:* These are the methods that are complete on their own, i.e., feature selection is a part of the algorithm. Variables are selected without splitting the data into training and testing subset (Chandrashekar & Sahin, 2014; Guyon & Elisseeff, 2003; Langley, 1994; Blum & Langley, 1997). We used a regularization method called the Least Absolute Shrinkage and Selection Operator (LASSO). It is a regression analysis method that adds a penalty to the least informative features to discard them thus avoiding overfitting.

(d) *Adaptive Heuristic Search Algorithm:* They are a time-saving approach to classical algorithms. Decision is made at each branching step by ranking the alternatives. *Genetic Algorithm (GA)* is one of the most advanced methods belonging to the class of Evolutionary Algorithms (EA). It is a stochastic method for feature optimization based on natural selection and genetics. It is a powerful selector (Salcedo-Sanz et al., 2004; Huang et al., 2007). GA uses three operators: selection, crossover and mutation to improve the quality of solutions. The estimator used here is linear regression, and the selector is GeneticSelectionCV. The scoring is based on the negative of the mean squared error.

Based on the above set of algorithms, we adopted CFS, Select K Best CFS, Select K Best MIFS, LASSO Regularization, RFECV and Genetic Algorithm in selecting the features from the Individual dataset and combined dataset.

Biomass from In Situ Data

To model the biomass of mangroves using remote sensing data, field biomass values of 42 sample plots were estimated using non-destructive methods since Bhitarkanika, being a National Park and Saltwater Crocodile Sanctuary, is protected by law. The biophysical measurements taken were used to estimate the plot biomass by the non-destructive sampling method using four species-specific and a common allometric equation (Table 2).

Statistical Analysis

The features' values of the three sensor type data were extracted for the co-located 3×3 kernel size of the field sample plots. Stepwise linear regression was performed to gauge the relationship between biomass and combined features for each dataset. We performed multiple regression analyses to model the AGB collected from in situ data against the features acquired from the 3 datasets namely (1) independent features extracted from individual data (2) Combination of features of each sensor (*Combine feature set*) (3) Combination of features from all 3 datasets, a multi-sensor approach (*Combined Dataset*). Stepwise regression was performed and a total of 48 features were obtained from all three sources combined after selecting the most informative

Table 2 Species-specific allometric equations used for the calculation of plot biomass

Sl. No.	Mangrove species	Species specific allometric equation	Source
1	*Avicennia marina*	$B = 0.308 \times DBH^{2.11}$	Comley & McGuinness, (2005)
2	*Bruguiera parviflora*	$B = 0.168 \times DBH^{2.42}$	Clough & Scott (1989)
3	*Pongamia pinnata*	$B = exp\{-2.409 + 0.9522\, ln\,(DBH^2 \times H \times \rho)\}$	(Ahmedin et al., 2013)
4	*Xylocarpus granatum*	$B = 0.0823 \times DBH^{2.59}$	Clough & Scott (1989)
5	*Common Mangrove*	$B = 0.251 \times \rho \times DBH2.46$	Komiyama et al. (2005)

H Tree Height, *DBH* Diameter at breast height, ρ wood density

features from all three datasets independently. All the regression analyses were carried out in python. The models for all three datasets were run for hundreds of times, dividing data into random training and test samples in the ratio of 80:20 to derive the regression coefficients for biomass estimation.

Results

AGB of mangrove forests of Bhitarkanika National Park was modeled using biomass estimated from the structural properties of the trees measured from 42 plots using allometric equations against varying spectral features derived from three sensor data namely SM, LO and AN having varied spectral and spatial resolution. In addition to the reflectance bands of each dataset, various other features such as band ratios, VIs and textural parameters were extracted to model the AGB based on the results of our earlier studies (Prasad & Gnanappazham, 2018).

Performance of the Independent Input Features from Each Satellite Data

When plot biomass was regressed with spectral reflectance, band ratios and VIs, band ratios of SM multispectral data performed better (R^2: 0.69) than LO multispectral data (R^2: 0.65) followed by VIs of AN. However, the LO Band Ratio has been modeled with the least RMSE of 321.80 t/ha. In general, band ratios reduce dispersion in simple reflectance bands caused by solar illumination, soil background and

topographic influences while also boosting spectral responsiveness from foliage. However, when textural parameters are introduced, the texture of VIs from LO yielded a better model (R^2: 0.44) followed by the texture of reflectance from SM ($R^2 = 0.41$). Textural parameters of reflectance, Band Ratios and VIs of all three sensor data were not found to improve the estimation when analyzed independently. Further, very high resolution AN was not found to give better results compared to medium and coarse resolution multispectral data. One of the reasons of this result could be the influence of textural transformation of the diverse canopy structure of very high-resolution data to model the biomass (Table 3).

Performance of the Combination of Input Features for Each Satellite Data

Since independent feature sets did not result satisfying outputs, we attempted modeling using a combination of all features (*Combined feature set*) like textural parameters of reflectance, band ratios, and VIs of each dataset LO, SM and AN with biomass. In this process about 20, 19 and 9 features were selected out of the combined feature set of AN, SM and LO, respectively (Table 4).

The results of step-wise linear regression analysis using a combination of all the six types of features found to improve the results for individual dataset in terms of RMSE rather than R^2 (Table 5). Our dataset has varying characteristics like LO is coarse resolution (multispectral) data, AN is

Table 3 Model fitting parameters derived from the results of biomass estimation using simple reflectance, band ratios, vegetation indices and textural parameters

Feature set	R^2			RMSE (t/ha)			F value		
	AN	SM	LO	AN	SM	LO	AN	SM	LO
Spectral Reflectance	0.27	0.07	0.17	450.78	486.29	432.18	0.88*	0.22	1.22*
Band ratios	Null	**0.69**	**0.65**	Null	614.10	321.80	Null	2.37	3.41
VIs	**0.50**	0.07	**0.41**	385.36	820.53	392.59	1.94	0.07*	1.95
Texture of reflectance	0.26	**0.41**	0.18	418.22	349.79	448.43	1.70*	9.04	0.96*
Texture of band ratio	Null	0.11	0.20	Null	757.92	402.95	Null	5.13	4.91
Texture of VIs	0.14	0.15	**0.44**	415.35	741.08	346.47	6.57	7.29	7.35

*insignificant models: Bold values represents the models with maximum R^2 values

Table 4 Selected features from combined feature set

Sensor	Code	Selected features
AVIRIS—NG	A1 (VI)	NDNI;
	A2–A20 (Texture)	Mean of B69, B178, NDLI, VREI2, PSRI and Red edge normalized ratio;
		Corr of ARI, NDVI, MSR and MTVI;
		Diss of ARI and TVI;
		Homo of B36 and TVI;
		Var of B98;
		Ent of SAVI and Water Index;
		Con of TVI and 2nd Moment of B62
Sentinel 2	S1–S3 (Reflectance)	B2_6; B4_5; B8A_11;
	S4–S19: (Texture)	Corr of B2 and B5_11;
		Con of B2, B6, B2_4, NDVI, RDVI and SAVI;
		Var of B12;
		Diss of DVI;
		2nd Moment of B6, B3_4, B6_7 and SAVI;
		Ent of B12 and B3_5
Landsat 8	L1–L9 (Texture)	Corr of B4_5 and EVI,
		Ent of B3, EVI and RDVI,
		2nd Moment of B4_7 and RDVI,
		Var of B4 and B2_3

Corr Correlation, *Diss* Dissimilarity, *Homo* Homogeneity, *Ent* Entropy, *Con* Contrast

(Two band numbers with underscore in between represent band ratio)

Table 5 Regression output for *combined feature set*

Sensor/satellite	R^2	RMSE (t/ha)	F value	Equation
AN	0.41	356.81	6.52	$2810.98 - 1404.00* A20 - 2910.15* A10 + 3667.20* A9 - 1119.51*A18$
LO	0.35	366.84	7.04	$-15{,}799.47 + 4873.03* L8 + 125{,}466.82* L6 - 1778.16* L9$
SM	0.85	195.49	16.42	$-6221.13 + 1823.45* S6 + 15{,}322.80* S14 + 74.39* S7 - 211{,}619.67* S16 + 99{,}510.48* S15 + 28{,}849.50* S17 + 76{,}449.63* S3 - 72{,}397.75* S2 - 33.40* S8 + 9230.19* S19 - 1788.38* S18$

high spatial and high spectral resolution (hyperspectral) data and Sentinel is medium spatial—spectral resolution data. Out of them, the model using SM is found to give better results (R^2: 0.85) with lesser RMSE (195.49 t/ha) than AN and LO showing similar results. It could be noted that the model has also retained more features from SM than AN and LO.

Performance of the *Combined Feature Set* from *Combined Sensor Datasets*

When the 48 selected features from all three datasets (LO, SM and AN) combined using different feature selection methods most of the methods selected a similar set of features from each data set (Table 6). Among them, K best MIFS selected a minimum of 4 features from AN and LO, while LASSO regression was not able to reduce the features (selected 40 features) from all three datasets. About 6 features were selected by RFECV from SM and LO ignoring AN.

Table 6 Identified features from regression analysis on *Combined Datasets*

Methods	Combined data set (AVIRIS + SM + LO)		
	AVIRIS	SM	LO
CFS	A15, A18, A9	S16	L8, L9
Select K best CFS	A18, A9	S16, S8	L8
Select K best MIFS	A1, A9	*No Selection*	L8, L9
LASSO regularization	A1–A20	S1, S3–S9, S11–S15, S17–S19	L4, L2, L8, L9
RFECV	*No Selection*	S1, S16, S3, S2	L3, L5–L7
GA	A12, A17	S5, S15	L8, L6, L9

While analyzing the model performance of the features selected by each of the methods, the least R^2 value was yielded by K Best CFS (0.15) with RMSE: 515.8 t/ha and the best out of 0.7 using GA (RMSE: 244.86 t/ha). Even though the features selected by RFECV could achieve an

Table 7 Regression output for selected features from *Combined Datasets*

Methods*	Combined Dataset of AN, SM and LO			
	R^2	RMSE (t/ha)	F value	Equation
CFS	0.38	360.12	4.39	$259.34 - 2.05*A15 - 9.38*A18 + 7.12*A9 + 13.60*L8 - 1087.93*L9$
Select K Best CFS	0.37	515.81	4.25	$2,382,973.47 - 6.23e+04*A18 + 2.07e+04*A9 + 1.15e+05*L8 - 1.20e+07*S16 - 1.04e+03*S8$
Select K Best MIFS	0.29	391.91	3.85	$6,032,441.72 - 1275.93*A1 + 35,194.56*A9 + 400,014.28*L8 - 205,093.73*L9$
RFECV	0.48	195.77	1.96	$-1226.86 - 595.69*L3 + 2764.19*L5 + 6428.61*L7 + 693.31*L6 - 285.43*S1 - 1024.03*S16 + 626.05*S3 + 544.23*S2$
LASSO	0.32	578.44	56.63	$704.69 + 0.005*A1 + 0.15*A2 \ldots + 11.92*S19$
GA	0.70	244.86	3.66	$-69.72 - 0.114*A12 - 18.288*A17 + 50.214*L8 + 1013.508*L6 - 19.459*L9 + 16.060*S5 + 627.44*S15$
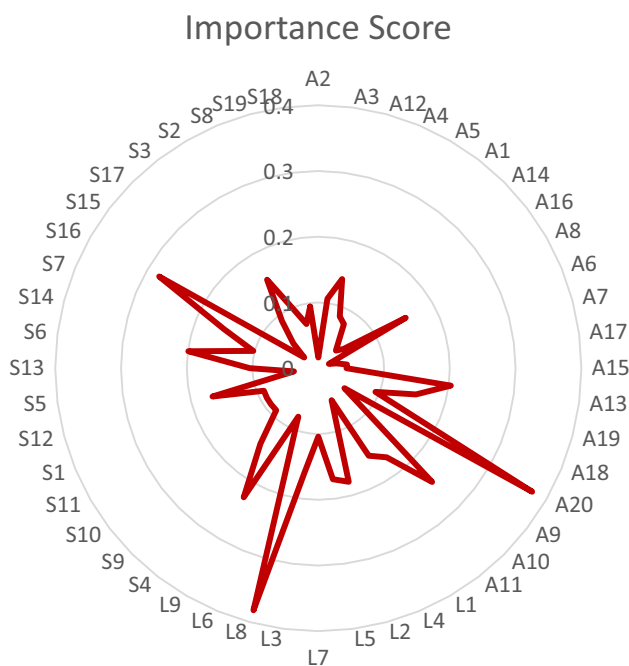
Fig. 3 Importance score of the Combined Data Set of AN, SM and LO

R^2 value of 0.48, the RMSE was found to be the lowest (195.778 t/ha) among all methods (Table 7).

The importance score of the *Combined feature set* for the analysis of the *Combined dataset* for all three data (Fig. 3) show that LO, A20 have the maximum score of 0.38 each and S16 with 0.28, respectively. Also, features from all sensors have comparatively similar scores as could be seen from the figure.

Discussion

It is well proven that textural parameters of multispectral satellite data yield better biomass estimation with more regression coefficient (Eckert, 2012; Zhu et al., 2015, Fuchs et al., 2009; Prasad & Gnanappazham, 2018). In our study on comparing varying spatial and spectral resolution also resulted that the textural features of all the basic features have been selected as the most contributing features for biomass estimation (Table 4) other than a few reflectance and a VI. However, when Individual data sets of each sensor was studied, the medium resolution multispectral data of Sentinel 2 was able to model with a higher coefficient of determination and lesser error (than coarse resolution (Landsat 8 OLI) and fine resolution hyperspectral data (AVIRIS-NG) (Fig. 4). Another important observation made was that all independent data sets were over estimating the biomass, while combined dataset estimates were closer to original though they are also overestimating. Notably the higher biomass values are mostly underestimated again substantiating the limitation of optical data. Sample Biomass map estimated using SM data of the study area is given for reference in Fig. 5. The multi-sensor approach could confirm the results what we were achieving independently for both hyper-spectral and multispectral data in terms of R^2 and RMSE in the estimation of biomass. All the feature selection methods had selected features from all three dataset except *Selected K Best MIFS* that yielded the least R^2 value. GA, the best of the models show that features from all sensors have equally contributed which is also evident from Fig. 3.

There are major challenges in estimating the biomass of mangroves using remote sensing methods. First, destructive methods from the sampled trees cannot be used to estimate the biomass due to the Act of the conservation and protection of National Parks and even any mangrove vegetation. Second, the availability of global allometric equations for estimating the ecologically sensitive vegetation types; (modeling of mangrove biomass is still dependent on allometric

Fig. 4 Comparison of estimated biomass from *Combined features set* and actual biomass estimated using allometry methods for **a** AN, **b** LO, **c** SM and **d** *Combined dataset*
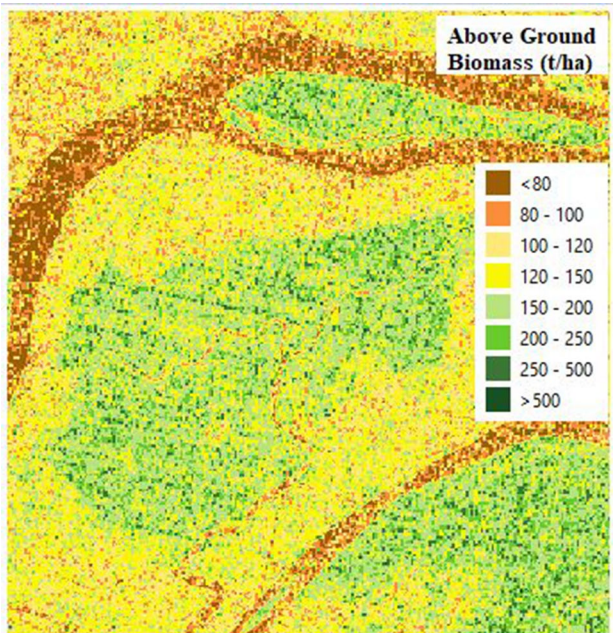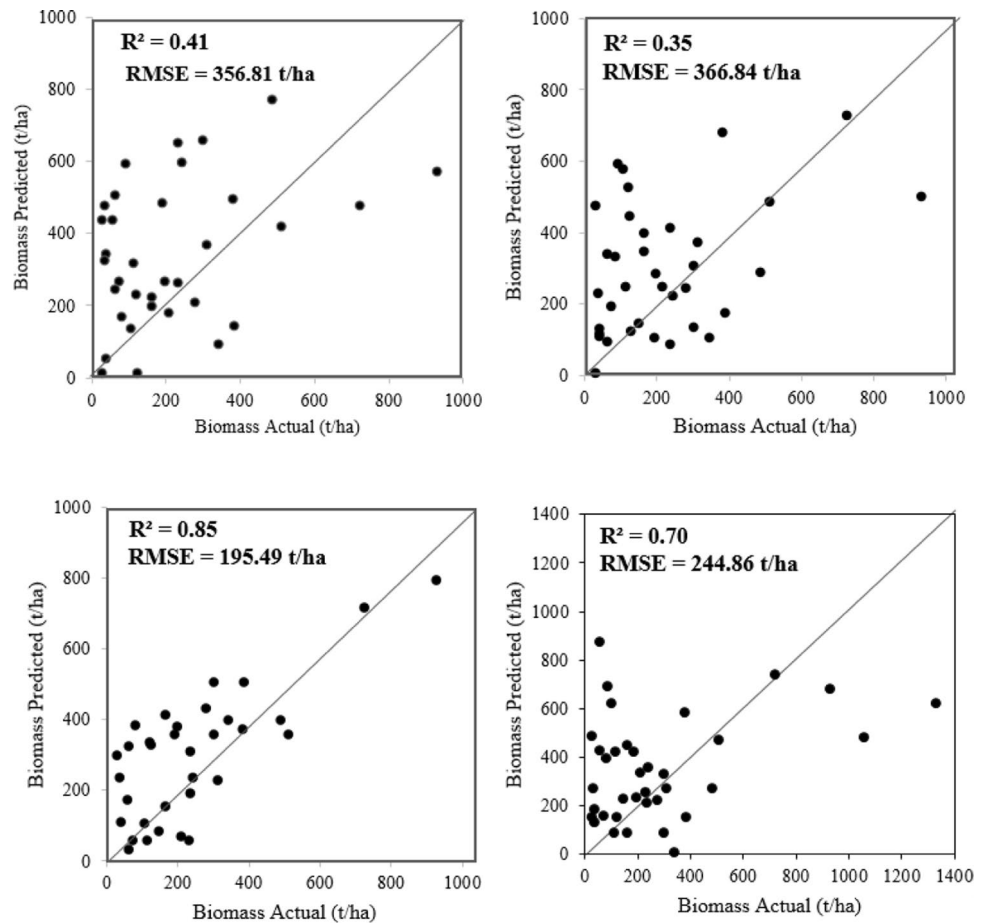

Fig. 5 Above-ground biomass estimated in the forest cover using combined feature set of Sentinel 2 Multispectral data

equations of global average only; Komiyama et al., 2005). Additionally, the species-specific allometric equations are available only for a few species. The present study of AGB estimation was also carried out with the above-mentioned challenges and lack of sufficient sample data on the mangrove structural parameters.

Beyond the data constraints, modeling the AGB of the mangroves using remote sensing data is also subjected to the prevailing structural complexity of the tropical evergreen forests (Sarker & Nichol, 2011). Utilizing or integrating Synthetic Aperture Radar data would probably lead to improved biomass modeling (Vaghela et al., 2021). Multifrequency analysis of Radar data was also found to be successful, wherein the canopy parameters sensed by low frequency radiations while sub canopy parameters by longer wavelengths making it effective in understanding the structure of the vegetation and its biomass (Proisy et al., 2003). Hence, a pertinently integrated framework of multisensory data will be able to overcome the uncertainties in the estimation of AGB of mangroves. Nevertheless, the uncertainties arising out of the non-availability of local specific allometric equation, usage of allometric methods for the actual biomass

estimation need to be addressed for the reliable estimation of AGB using remote sensing methods.

Conclusion

Our study was a preliminary study that shows the trend in the modeling of AGB using features from different types of sensors—multispectral and hyperspectral independently as well as in a multi-sensor approach. Site-specific results show that the multi-sensor approach has not improved the biomass estimation of the independent sensor. Use of Visible and Near InfraRed range of spectrum would have resulted in similar results, however, the features selection method of the Genetic Algorithm on medium resolution multispectral data has given the best result in our study. The research also indicated that the incorporation of textural features improved the R^2 values. This can be as texture might link to the fractional vegetation canopy (FVC) of the tree, which is now known to be an estimator of biomass. The future studies may integrate data from more sensors like SAR and LiDAR to have a better understanding of the multi-sensor approach for the estimation of AGB of mangroves.

Declarations

References

Ahmedin, A. M., Bam, S., Siraj, K. T., & Raju, A. S. (2013). Assessment of biomass and carbon sequestration potentials of standing Pongamia pinnata in Andhra University, Visakhapatnam. *India. Bioscience Discovery, 4*(2), 143–148.

Alongi, D. M. (2002). Present state and future of the World's mangrove forests. *Environmental Conservation, 29*(3), 331–349. https://doi.org/10.1017/S0376892902000231

Alongi, D. M., & Mukhopadhyay, S. K. (2015). Contribution of mangroves to coastal carbon cycling in low latitude seas. *Agricultural and Forest Meteorology, 213*, 266–272. https://doi.org/10.1016/j.agrformet.2014.10.005

Alongi, D. M., Wattayakorn, G., Boyle, S., Tirendi, F., Payn, C., & Dixon, P. (2004). Influence of roots and climate on mineral and trace element storage and flux in tropical mangrove soils. *Biogeochemistry, 69*(1), 105–123.

Armi, L., & Fekri-Ershad, S. (2019). Texture image analysis and texture classification methods-A review. arXiv:1904.06554. https://doi.org/10.48550/arXiv.1904.06554

Arun Prasad, K., & Gnanappazham, L. (2014). Species discrimination of mangroves using derivative spectral analysis. *ISPRS Annals of the Photogrammetry, Remote Sensing and Spatial Information Sciences, 2*, 45–52. https://doi.org/10.5194/isprsannals-II-8-45-2014

Blum, A. L., & Langley, P. (1997). Selection of relevant features and examples in machine learning. *Artificial Intelligence, 97*(1–2), 245–271. https://doi.org/10.1016/S0004-3702(97)00063-5

Bouillon, S., Borges, A. V., Castañeda-Moya, E., Diele, K., Dittmar, T., Duke, N. C., Kristensen, E., Lee, S. Y., Marchand, C., Middelburg, J. J., & Rivera-Monroy, V. H. (2008). Mangrove production and carbon sinks: A revision of global budget estimates. *Global biogeochemical cycles*. https://doi.org/10.1029/2007GB003052

Boyd, D. S., & Danson, F. M. (2005). Satellite remote sensing of forest resources: Three decades of research development. *Progress in Physical Geography, 29*(1), 1–26. https://doi.org/10.1191/0309133305pp432ra

Broge, N. H., & Leblanc, E. (2001). Comparing prediction power and stability of broadband and hyperspectral vegetation indices for estimation of green leaf area index and canopy chlorophyll density. *Remote Sensing of Environment, 76*(2), 156–172. https://doi.org/10.1016/S0034-4257(00)00197-8

Bue, B. D., Thompson, D. R., Eastwood, M., Green, R. O., Gao, B. C., Keymeulen, D., Sarture, C. M., Mazer, A. S., & Luong, H. H. (2015). Real-time atmospheric correction of AVIRIS-NG imagery. *IEEE Transactions on Geoscience and Remote Sensing, 53*(12), 6419–6428.

Calvao, T., & Palmeirim, J. M. (2004). Mapping Mediterranean scrub with satellite imagery: Biomass estimation and spectral behaviour. *International journal of remote sensing, 25*(16), 3113–3126. https://doi.org/10.1109/TGRS.2015.2439215

Castel, T., Guerra, F., Caraglio, Y., & Houllier, F. (2002). Retrieval biomass of a large Venezuelan pine plantation using JERS-1 SAR data. Analysis of forest structure impact on radar signature. *Remote Sensing of Environment, 79*(1), 30–41. https://doi.org/10.1016/S0034-4257(01)00236-X

Champagne, C., Pattey, E., Bannari, A., & Strachan, I. B. (2001). Mapping crop water stress: issues of scale in the detection of plant water status using hyperspectral indices. In *Mesures physiques et signatures en télédétection (Aussois, 8–12 January 2001)* (pp. 79–84).

Chandrashekar, G., & Sahin, F. (2014). A survey on feature selection methods. *Computers & Electrical Engineering, 40*(1), 16–28. https://doi.org/10.1016/j.compeleceng.2013.11.024

Chaube, N. R., Lele, N., Misra, A., Murthy, T. V. R., Manna, S., Hazra, S., Panda, M., & Samal, R. N. (2019). Mangrove species discrimination and health assessment using AVIRIS-NG hyperspectral data. *Current Science, 116*(7), 1136–1142.

Chave, J., Coomes, D., Jansen, S., Lewis, S. L., Swenson, N. G., & Zanne, A. E. (2009). Towards a worldwide wood economics spectrum. *Ecology Letters, 12*(4), 351–366. https://doi.org/10.1111/j.1461-0248.2009.01285.x

Chen, D., Stow, D. A., & Gong, P. (2004). Examining the effect of spatial resolution and texture window size on classification accuracy:

an urban environment case. *International Journal of Remote Sensing, 25*(11), 2177–2192.

Chen, J. M. (1996). Evaluation of vegetation indices and a modified simple ratio for boreal applications. *Canadian Journal of Remote Sensing, 22*(3), 229–242. https://doi.org/10.1080/07038992.1996.10855178

Clough, B. F., & Scott, K. (1989). Allometric relationships for estimating above-ground biomass in six mangrove species. *Forest Ecology and Management, 27*(2), 117–127. https://doi.org/10.1016/0378-1127(89)90034-0

Comley, B. W., & McGuinness, K. A. (2005). Above-and below-ground biomass, and allometry, of four common northern Australian mangroves. *Australian Journal of Botany, 53*(5), 431–436. https://doi.org/10.1071/BT04162

Daughtry, C. S., Walthall, C. L., Kim, M. S., De Colstoun, E. B., & McMurtrey Iii, J. E. (2000). Estimating corn leaf chlorophyll concentration from leaf and canopy reflectance. *Remote Sensing of Environment, 74*(2), 229–239. https://doi.org/10.1016/S0034-4257(00)00113-9

Dell'Acqua, F., & Gamba, P. (2006). Discriminating urban environments using multiscale texture and multiple SAR images. *International Journal of Remote Sensing, 27*(18), 3797–3812. https://doi.org/10.1080/01431160600557572

Dobson, M. C., Ulaby, F. T., Pierce, L. E., Sharik, T. L., Bergen, K. M., Kellndorfer, J., Kendra, J. R., Li, E., Lin, Y. C., Nashashibi, A., & Sarabandi, K. (1995). Estimation of forest biophysical characteristics in Northern Michigan with SIR-C/X-SAR. *IEEE Transactions on Geoscience and Remote Sensing, 33*(4), 877–895. https://doi.org/10.1109/36.406674

Dunne, K., Cunningham, P., & Azuaje, F. (2002). Solutions to instability problems with sequential wrapper-based approaches to feature selection. *Journal of Machine Learning Research, 1*, 22.

DW, D. (1975). Measuring forage production of grazing units from Landsat MSS data. In *Proceedings of 10th international symposium on remote sensing of environment, 1975* (pp. 1169–1178). ERIM.

Eckert, S. (2012). Improved forest biomass and carbon estimations using texture measures from WorldView-2 satellite data. *Remote Sensing, 4*(4), 810–829. https://doi.org/10.3390/rs4040810

Elvidge, C. D., & Chen, Z. (1995). Comparison of broad-band and narrow-band red and near-infrared vegetation indices. *Remote Sensing of Environment, 54*(1), 38–48. https://doi.org/10.1016/0034-4257(95)00132-K

Espinoza-Tenorio, A., Millán-Vásquez, N. I., Vite-García, N., & Alcalá-Moya, G. (2019). People and blue carbon: Conservation and settlements in the mangrove forests of Mexico. *Human Ecology, 47*, 877–892.

Fatoyinbo, T. E., Simard, M., Washington-Allen, R. A., & Shugart, H. H. (2008). Landscape-scale extent, height, biomass, and carbon estimation of Mozambique's mangrove forests with Landsat ETM+ and Shuttle Radar Topography Mission elevation data. *Journal of Geophysical Research: Biogeosciences.* https://doi.org/10.1029/2007JG000551

Foody, G. M., Cutler, M. E., McMorrow, J., Pelz, D., Tangki, H., Boyd, D. S., & Douglas, I. A. N. (2001). Mapping the biomass of Bornean tropical rain forest from remotely sensed data. *Global Ecology and Biogeography, 10*(4), 379–387. https://doi.org/10.1046/j.1466-822X.2001.00248.x

Fuchs, H., Magdon, P., Kleinn, C., & Flessa, H. (2009). Estimating aboveground carbon in a catchment of the Siberian forest tundra: Combining satellite imagery and field inventory. *Remote Sensing of Environment, 113*(3), 518–531. https://doi.org/10.1016/j.rse.2008.07.017

Gitelson, A. A. (2004). Wide dynamic range vegetation index for remote quantification of biophysical characteristics of vegetation.

Journal of Plant Physiology, 161(2), 165–173. https://doi.org/10.1078/0176-1617-01176

Gitelson, A. A., Keydan, G. P., & Merzlyak, M. N. (2006). Three-band model for noninvasive estimation of chlorophyll, carotenoids, and anthocyanin contents in higher plant leaves. *Geophysical research letters.* https://doi.org/10.1029/2006GL026457

Green, E. P., Clark, C. D., Mumby, P. J., Edwards, A. J., & Ellis, A. C. (1998). Remote sensing techniques for mangrove mapping. *International Journal of Remote Sensing, 19*(5), 935–956. https://doi.org/10.1080/014311698215801

Guyon, I., & Elisseeff, A. (2003). An introduction to variable and feature selection. *Journal of machine learning research, 3*(Mar), 1157–1182.

Haboudane, D., Miller, J. R., Pattey, E., Zarco-Tejada, P. J., & Strachan, I. B. (2004). Hyperspectral vegetation indices and novel algorithms for predicting green LAI of crop canopies: Modeling and validation in the context of precision agriculture. *Remote Sensing of Environment, 90*(3), 337–352. https://doi.org/10.1016/j.rse.2003.12.013

Hame, T., Salli, A., Andersson, K., & Lohi, A. (1997). A new methodology for the estimation of biomass of coniferdominated boreal forest using NOAA AVHRR data. *International Journal of Remote Sensing, 18*(15), 3211–3243. https://doi.org/10.1080/014311697217053

Haralick, R. M. (1979). Statistical and structural approaches to texture. *Proceedings of the IEEE, 67*(5), 786–804. https://doi.org/10.1109/PROC.1979.11328

Haralick, R. M., Shanmugam, K., & Dinstein, I. H. (1973). Textural features for image classification. *IEEE Transactions on Systems, Man, and Cybernetics, 6*, 610–621. https://doi.org/10.1109/TSMC.1973.4309314

Haury, A. C., Gestraud, P., & Vert, J. P. (2011). The influence of feature selection methods on accuracy, stability and interpretability of molecular signatures. *PLoS ONE, 6*(12), e28210. https://doi.org/10.1371/journal.pone.0028210

Hirata, Y., Tabuchi, R., Patanaponpaiboon, P., Poungparn, S., Yoneda, R., & Fujioka, Y. (2014). Estimation of aboveground biomass in mangrove forests using high-resolution satellite data. *Journal of Forest Research, 19*(1), 34–41. https://doi.org/10.1007/s10310-013-0402-5

Horler, D. N. H., Dockray, M., & Barber, J. (1983). The red edge of plant leaf reflectance. *International Journal of Remote Sensing, 4*(2), 273–288. https://doi.org/10.1080/01431168308948546

Huang, J., Cai, Y., & Xu, X. (2007). A hybrid genetic algorithm for feature selection wrapper based on mutual information. *Pattern Recognition Letters, 28*(13), 1825–1844. https://doi.org/10.1016/j.patrec.2007.05.011

Huete, A. R., Liu, H., & van Leeuwen, W. J. (1997). The use of vegetation indices in forested regions: issues of linearity and saturation. In *IGARSS'97. 1997 IEEE international geoscience and remote sensing symposium proceedings. Remote sensing-a scientific vision for sustainable development* (vol. 4, pp. 1966–1968). IEEE. https://doi.org/10.1109/IGARSS.1997.609169

Huete, A. R. (1988). A soil-adjusted vegetation index (SAVI). *Remote Sensing of Environment, 25*(3), 295–309. https://doi.org/10.1016/0034-4257(88)90106-X

Hunt, E. R., Jr., & Rock, B. N. (1989). Detection of changes in leaf water content using near-and middle-infrared reflectances. *Remote Sensing of Environment, 30*(1), 43–54. https://doi.org/10.1016/0034-4257(89)90046-1

Hyde, P., Nelson, R., Kimes, D., & Levine, E. (2007). Exploring LiDAR–RaDAR synergy—predicting aboveground biomass in a southwestern ponderosa pine forest using LiDAR, SAR and InSAR. *Remote Sensing of Environment, 106*(1), 28–38. https://doi.org/10.1016/j.rse.2006.07.017

Kalousis, A., Prados, J., & Hilario, M. (2007). Stability of feature selection algorithms: A study on high-dimensional spaces. *Knowledge and Information Systems, 12*, 95–116.

Kasawani, I., Norsaliza, U., & Mohdhasmadi, I. (2010). Analysis of spectral vegetation indices related to soil-line for mapping mangrove forests using satellite imagery.

Kaufman, Y. J., & Tanre, D. (1992). Atmospherically resistant vegetation index (ARVI) for EOS-MODIS. *IEEE Transactions on Geoscience and Remote Sensing, 30*(2), 261–270. https://doi.org/10.1109/36.134076

Kim, M. S., Daughtry, C. S. T., Chappelle, E. W., McMurtrey, J. E., & Walthall, C. L. (1994). The use of high spectral resolution bands for estimating absorbed photosynthetically active radiation (A par). In *CNES, proceedings of 6th international symposium on physical measurements and signatures in remote sensing* (No. GSFC-E-DAA-TN72921).

Komiyama, A., Poungparn, S., & Kato, S. (2005). Common allometric equations for estimating the tree weight of mangroves. *Journal of Tropical Ecology, 21*(4), 471–477.

Kovacs, J. M., King, J. M. L., Flores de Santiago, F., & Flores-Verdugo, F. (2009). Evaluating the condition of a mangrove forest of the Mexican Pacific based on an estimated leaf area index mapping approach. *Environmental Monitoring and Assessment, 157*, 137–149. https://doi.org/10.1007/s10661-008-0523-z

Kristensen, E., Bouillon, S., Dittmar, T., & Marchand, C. (2008). Organic carbon dynamics in mangrove ecosystems: A review. *Aquatic Botany, 89*(2), 201–219. https://doi.org/10.1016/j.aquabot.2007.12.005

Kuplich, T. M., Curran, P. J., & Atkinson, P. M. (2005). Relating SAR image texture to the biomass of regenerating tropical forests. *International Journal of Remote Sensing, 26*(21), 4829–4854. https://doi.org/10.1080/01431160500239107

Kurvonen, L., Pulliainen, J., & Hallikainen, M. (1999). Retrieval of biomass in boreal forests from multitemporal ERS-1 and JERS-1 SAR images. *IEEE Transactions on Geoscience and Remote Sensing, 37*(1), 198–205. https://doi.org/10.1109/36.739154

Langley, P. (1994). Selection of relevant features in machine learning In *Proceedings of the AAAI fall symposium on relevance*. AAAI.

Liang, S. (2005). *Quantitative remote sensing of land surfaces*. Wiley.

Merzlyak, M. N., Gitelson, A. A., Chivkunova, O. B., & Rakitin, V. Y. (1999). Non-destructive optical detection of pigment changes during leaf senescence and fruit ripening. *Physiologia Plantarum, 106*(1), 135–141. https://doi.org/10.1034/j.1399-3054.1999.106119.x

Mutanga, O., & Skidmore, A. K. (2004). Narrow band vegetation indices overcome the saturation problem in biomass estimation. *International Journal of Remote Sensing, 25*(19), 3999–4014. https://doi.org/10.1080/01431160310001654923

Nagelkerken, I. S. J. M., Blaber, S. J. M., Bouillon, S., Green, P., Haywood, M., Kirton, L. G., Meynecke, J. O., Pawlik, J., Penrose, H. M., Sasekumar, A., & Somerfield, P. J. (2008). The habitat function of mangroves for terrestrial and marine fauna: A review. *Aquatic Botany, 89*(2), 155–185. https://doi.org/10.1016/j.aquabot.2007.12.007

Nellis, M. D., & Briggs, J. M. (1992). Transformed vegetation index for measuring spatial variation in drought impacted biomass on Konza Prairie, Kansas. *Transactions of the Kansas Academy of Science, 1903*, 93–99. https://doi.org/10.2307/3628024

Nichol, J. E., & Sarker, M. L. R. (2010). Improved biomass estimation using the texture parameters of two high-resolution optical sensors. *IEEE Transactions on Geoscience and Remote Sensing, 49*(3), 930–948. https://doi.org/10.1109/TGRS.2010.2068574

Patil, V., Singh, A., Naik, N., & Unnikrishnan, S. (2014). Estimation of carbon stocks in *Avicennia marina* stand using allometry, CHN analysis, and GIS methods. *Wetlands, 34*, 379–391.

Podest, E., & Saatchi, S. (2002). Application of multiscale texture in classifying JERS-1 radar data over tropical vegetation. *International Journal of Remote Sensing, 23*(7), 1487–1506. https://doi.org/10.1080/01431160110093000

Prasad, a. (2016). *Spectral analysis for the species characterization of mangroves of Bhitarkanika national park, Odisha, India using hyperspectral remote sensing* (doctoral dissertation, Indian institute of space science and technology).

Prasad, K. A., & Gnanappazham, L. (2018). Estimation of above ground biomass using high resolution multispectral worldview 2 image. *Indian Cartographer, 38*, 569–579.

Proisy, C., Mitchell, A., Lucas, R., Fromard, F., & Mougin, E. (2003, May). Estimation of mangrove biomass using multifrequency radar data. Application to mangroves of French Guiana and Northern Australia. In *Proceedings of the Mangrove 2003 conference* (pp. 20–24).

Pu, R., & Landry, S. (2012). A comparative analysis of high spatial resolution IKONOS and WorldView-2 imagery for mapping urban tree species. *Remote Sensing of Environment, 124*, 516–533. https://doi.org/10.1016/j.rse.2012.06.011

Qi, J., Chehbouni, A., Huete, A. R., Kerr, Y. H., & Sorooshian, S. (1994). A modified soil adjusted vegetation index. *Remote Sensing of Environment, 48*(2), 119–126. https://doi.org/10.1016/0034-4257(94)90134-1

Ravishankar, T., Navamuniyammal, M., Gnanappazham, L., Nayak, S. S., Mahapatra, G. C., & Selvam, V. (2004). Atlas of mangrove wetlands of India. Part 3: Orissa.

Rock, B. N., Vogelmann, J. E., Williams, D. L., Vogelmann, A. F., & Hoshizaki, T. (1986). Remote detection of forest damage. *BioScience, 36*(7), 439–445. https://doi.org/10.2307/1310339

Rondeaux, G., Steven, M., & Baret, F. (1996). Optimization of soil-adjusted vegetation indices. *Remote Sensing of Environment, 55*(2), 95–107. https://doi.org/10.1016/0034-4257(95)00186-7

Roujean, J. L., & Breon, F. M. (1995). Estimating PAR absorbed by vegetation from bidirectional reflectance measurements. *Remote Sensing of Environment, 51*(3), 375–384. https://doi.org/10.1016/0034-4257(94)00114-3

SAC. (2012). *Coastal Zones of India*. Space Application Centre (ISRO).

Salcedo-Sanz, S., & Yao, X. (2004). A hybrid Hopfield network-genetic algorithm approach for the terminal assignment problem. *IEEE Transactions on Systems, Man, and Cybernetics, Part B (Cybernetics), 34*(6), 2343–2353. https://doi.org/10.1109/TSMCB.2004.836471

Santos, J. R., Freitas, C. C., Araujo, L. S., Dutra, L. V., Mura, J. C., Gama, F. F., Soler, L. S., & Sant'Anna, S. J. (2003). Airborne P-band SAR applied to the aboveground biomass studies in the Brazilian tropical rainforest. *Remote Sensing of Environment, 87*(4), 482–493. https://doi.org/10.1016/j.rse.2002.12.001

Sarker, L. R., & Nichol, J. E. (2011). Improved forest biomass estimates using ALOS AVNIR-2 texture indices. *Remote Sensing of Environment, 115*(4), 968–977. https://doi.org/10.1016/j.rse.2010.11.010

Serrano, L., Penuelas, J., & Ustin, S. L. (2002). Remote sensing of nitrogen and lignin in Mediterranean vegetation from AVIRIS data: Decomposing biochemical from structural signals. *Remote Sensing of Environment, 81*(2–3), 355–364. https://doi.org/10.1016/S0034-4257(02)00011-1

Sims, D. A., & Gamon, J. A. (2002). Relationships between leaf pigment content and spectral reflectance across a wide range of species, leaf structures and developmental stages. *Remote Sensing of Environment, 81*(2–3), 337–354. https://doi.org/10.1016/S0034-4257(02)00010-X

Somol, P., & Novovičová, J. (2010). Evaluating stability and comparing output of feature selectors that optimize feature subset cardinality.

IEEE Transactions on Pattern Analysis and Machine Intelligence, 32(11), 1921–1939. https://doi.org/10.1109/TPAMI.2010.34

Steininger, M. K. (2000). Satellite estimation of tropical secondary forest above-ground biomass: Data from Brazil and Bolivia. *International Journal of Remote Sensing, 21*(6–7), 1139–1157. https://doi.org/10.1080/014311600210119

Tuceryan, M., & Jain, A. K. (1993). Texture analysis. In C. H. Chen (Ed.), *Handbook of pattern recognition and computer vision* (pp. 235–276). World scientific. https://doi.org/10.1142/9789814343138_0010

Tucker, C. J. (1979). Red and photographic infrared linear combinations for monitoring vegetation. *Remote Sensing of Environment, 8*(2), 127–150. https://doi.org/10.1016/0034-4257(79)90013-0

Ulaby, F. T., Kouyate, F., Brisco, B., & Williams, T. L. (1986). Textural information in SAR images. *IEEE Transactions on Geoscience and Remote Sensing, 2*, 235–245. https://doi.org/10.1109/TGRS.1986.289643

Vaghela, B., Chirakkal, S., Putrevu, D., & Solanki, H. (2021). Modelling above ground biomass of Indian mangrove forest using dual-pol SAR data. *Remote Sensing Applications: Society and Environment, 21*, 100457. https://doi.org/10.1016/j.rsase.2020.100457

Venkatesh, B., & Anuradha, J. (2019). A review of feature selection and its methods. *Cybernetics and Information Technologies, 19*(1), 3–26. https://doi.org/10.2478/cait-2019-0001

Vogelmann, J. E., Rock, B. N., & Moss, D. M. (1993). Red edge spectral measurements from sugar maple leaves. *TitleREMOTE SENSING, 14*(8), 1563–1575. https://doi.org/10.1080/01431169308953986

Woodcock, C. E., & Strahler, A. H. (1987). The factor of scale in remote sensing. *Remote Sensing of Environment, 21*(3), 311–332. https://doi.org/10.1016/0034-4257(87)90015-0

Yang, F., & Mao, K. Z. (2011). Robust feature selection for microarray data based on multicriterion fusion. *IEEE/ACM Transactions on Computational Biology and Bioinformatics, 8*(4), 1080–1092. https://doi.org/10.1109/TCBB.2010.103

Zanne, A.E., Lopez-Gonzalez, G., Coomes, D.A., Ilic, J., Jansen, S., Lewis, S.L., Miller, R.B., Swenson, N.G., Wiemann, M.C. & Chave, J., 2020. Data from: Towards a worldwide wood economics spectrum. https://doi.org/10.5061/dryad.234

Zhu, Y., Liu, K., Liu, L., Wang, S., & Liu, H. (2015). Retrieval of mangrove aboveground biomass at the individual species level with worldview-2 images. *Remote Sensing, 7*(9), 12192–12214. https://doi.org/10.3390/rs70912192